Dyes and Pigments 95 (2012) 644–656

Contents lists available at SciVerse ScienceDirect

Dyes and Pigments

journal homepage: www.elsevier.com/locate/dyepig

Synthesis, crystal structure and spectroscopic study of novel benzimidazoles and benzimidazo[1,2-*a*]quinolines as potential chemosensors for different cations

Marijana Hranjec [a,*], Ema Horak [a], Martina Tireli [a], Gordana Pavlović [b], Grace Karminski-Zamola [a]

[a] Department of Organic Chemistry, Faculty of Chemical Engineering and Technology, University of Zagreb, Marulićev trg 19, P. O. Box 177, HR-10000 Zagreb, Croatia
[b] Faculty of Textile Technology, Department of Applied Chemistry, University of Zagreb, Prilaz baruna Filipovića 28a, HR-10000 Zagreb, Croatia

ARTICLE INFO

Article history:
Received 23 March 2012
Received in revised form
22 May 2012
Accepted 23 May 2012
Available online 13 July 2012

Keywords:
Benzimidazoles
Benzimidazo[1,2-*a*]quinolines
Crystal structure
UV/Vis and fluorescence spectroscopy
Chemosensors
Zinc

ABSTRACT

In this manuscript the synthesis, crystal structure, spectroscopic characterization and titration with several metal chloride salts of novel *E*-3-phenyl-2-(1-phenylbenzimidazol-2-yl)acrylonitriles and 5-phenylbenzimidazo[1,2-*a*]quinoline derivatives are described. All compounds were characterized by means of ^{1}H, ^{13}C NMR, MS, UV/Vis and fluorescence spectroscopy.

Crystal and molecular structures of *E*-3-(4-nitrophenyl)-2-(1-phenyl-benzimidazol-2-yl)acrylonitrile and 5-phenylbenzimidazo[1,2-*a*]quinoline-6-carbonitrile were determined by single-crystal X-ray diffractometry. The molecular assembly is characterized by the C–H···O and C–H···N intermolecular hydrogen bonds in *E*-3-(4-nitrophenyl)-2-(1-phenyl-benzimidazol-2-yl)acrylonitrile and 5-phenylbenzimidazo [1,2-*a*]quinoline-6-carbonitrile, respectively.

Spectroscopic characterization of the prepared compounds was performed by using UV/Vis and fluorescence spectroscopy in ethanol. In order to determine a selectivity towards a variety of cations, to explore their use as potential chemosensors, the amino substituted 5-phenylbenzimidazo[1,2-*a*]quinoline-6-carbonitrile was chosen for a titration with metal chloride salts using fluorescence spectroscopy. The fluorescence intensity significantly increased upon addition of Zn^{2+} and Ag^{+} cations while decreased by addition of Mn^{2+}, Co^{2+}, Cu^{2+}, Hg^{2+}, Li^{+} and Fe^{3+} cations.

1. Introduction

The permanent and growing interest in recent years for the synthesis of sensitive and selective chemosensors that are capable of assaying cations or anions in solution is a direct consequence of their great importance in the areas of biological, medicinal and environmental science [1–3]. Heterocyclic sensors with excellent spectroscopic properties, capable of detecting versatile ions with different spectral responses, have been one of the most extensively studied classes of organic compounds [4,5]. Fluorescence spectroscopy as a very sensitive, efficient and economic method has been widely used for a quantification of biologically important ions [6]. Fluorescent sensors have many advantages including high sensitivity, easy availability and possible multiple modes of detection like fluorescence quenching and enhancing or fluorescence lifetime [7,8]. Usually, a typical fluorescent chemosensor contains a recognition site linked to a fluorophore as the signal source which translates the recognition event into the fluorescence signal [9].

The benzimidazole unit is one of the most important key building blocks for a variety of compounds which have crucial roles in the functions of biologically important molecules [10,11]. Mostly, benzimidazole derivatives display diverse biological activities such as antibacterial [12,13], antitumor [14–16], antifungal [17] or antiviral [18] and furthermore due to the structural similarity of benzimidazole nuclei with naturally occurring compounds such as purine, they can easily interact with biomolecules of the living systems [10]. Besides, benzimidazoles have found applications in several other areas such as optical lasers and polymer dyes in optoelectronics [19,20], fluorescent probes for detection of biological important molecules as DNA, RNA or proteins in biomedical diagnostics [21,22], efficient and selective chemosensors for cation or anion detection [23,24] and as efficient ligands in metallochemistry [25]. Benzannulated benzimidazole analogues such as benzimidazo[1,2-*a*]quinolines, are highly conjugated planar chromophores and very important fluorophores with excellent spectroscopic characteristics including high fluorescence intensity which is very important in their possible application as fluorescent probes in homogeneous assays of biological molecules [26,27].

* Corresponding author. Department of Organic Chemistry, Faculty of Chemical Engineering and Technology, University of Zagreb, Marulićev trg 20, P.O. Box 177, HR-10000 Zagreb, Croatia. Tel.: +385 14597245; fax: +385 14597250.
E-mail address: mhranjec@fkit.hr (M. Hranjec).

0143-7208/$ – see front matter © 2012 Elsevier Ltd. All rights reserved.
http://dx.doi.org/10.1016/j.dyepig.2012.05.024

Additionally, fluorescence can be significantly altered by additional substituents placed on different positions of the planar chromophore. We have recently reported on the synthesis of amino substituted benzimidazo[1,2-*a*]quinolines which significantly enhanced fluorescence emission intensity upon addition of calf thymus DNA and thus offer the potential applications as a DNA-specific fluorescent probes [28].

Prompted by the aforementioned considerations and as a part of our continuing research on the synthesis and spectroscopic characterization of benzimidazole derivatives, we set out to explore and synthesize novel acyclic *E*-3-phenyl-2-(1-phenylbenzimidazol-2-yl)acrylonitriles and 5-phenyl-benzimidazo[1,2-*a*]quinolines. The prepared compounds were characterized by means of UV/Vis and fluorescence spectroscopy while amino substituted 5-phenyl-benzimidazo[1,2-*a*]quinoline **5** was investigated as a potential chemosensor, by fluorescence spectroscopy in the presence of several metal chloride salts to determine its selectivity towards versatile cations. Compound **5** showed the highest enhancement of fluorescence intensity in the presence of Zn^{2+} cations and almost the total quenching of fluorescence intensity in the presence of Cu^{2+} cations.

2. Experimental

2.1. General methods

All chemicals and solvents were purchased from commercial suppliers Acros, Aldrich or Fluka. Melting points were recorded on SMP11 Bibby and Büchi 535 apparatus. The ^{1}H and ^{13}C NMR spectra were recorded on a Varian Gemini 300 or Varian Gemini 600 at 300, 600 and 150 and 75 MHz, respectively. All NMR spectra were measured in DMSO-d_6 solutions using TMS as an internal standard. Chemical shifts are reported in ppm (δ) relative to TMS. In preparative photochemical experiments the irradiation was performed at room temperature with a water-cooled immersion well with "Origin Hanau" 400-W high pressure mercury arc lamp using Pyrex glass as a cut-off filter of wavelengths below 280 nm. Mass spectra were recorded on an Agilent 1200 series LC/6410 QQQ instrument. The electronic absorption spectra were recorded on Varian Cary 50 spectrometer using quartz cuvette (1 cm). All compounds were routinely checked by TLC with Merck silica gel 60F-254 glass plates. Elemental analysis for carbon, hydrogen and nitrogen were performed on a Perkin–Elmer 2400 elemental analyzer. Where analyses are indicated only as symbols of elements, analytical results obtained are within 0.4% of the theoretical value.

2.2. Synthesis

2.2.1. 2-Cyanomethyl-N-phenylbenzimidazole **1**

A mixture of equimolar amounts of *N*-phenyl-1,2-phenylenediamine (3.00 g, 16.30 mmol) and 2-cyanoacetamide (2.70 g, 16.30 mmol) was heated in an oil bath for 20 min at 200 °C. After cooling, the reaction mixture was treated with 50% ethanol/water (100 mL) and resulting product was filtered off. After recrystallization from ethanol/water the green crystals (2.50 g, 66%) obtained. m.p. 118–120 °C; ^{1}H NMR (300 MHz, DMSO-d_6): δ = 7.76 (dd, 1H, J_1 = 6.90 Hz, J_2 = 2.07 Hz, $H_{arom.}$), 7.69–7.62 (m, 3H, H_{arom}), 7.58 (d, 2H, J = 7.10 Hz, $H_{arom.}$), 7.31–7.27 (m, 2H, H_{arom}), 7.16 (dd, 1H, J_1 = 6.93 Hz, J_2 = 2.31 Hz), 4.37 (s, 2H, CH_2); MS (*m*/*z*): 233 ($[M]^+$); UV (EtOH) λ_{max}: 338.

2.2.2. General procedure for synthesis of compounds **3a**–**3e**

A solution of equimolar amounts of 2-cyanomethyl-*N*-phenylbenzimidazole **1**, corresponding heteroaromatic aldehydes **2a**–**2e** and a few drops of piperidine in absolute ethanol, were refluxed for 3–3.5 h. After reaction mixture was cooled to the room temperature, the crude product was filtered off and recrystallized from ethanol.

2.2.2.1. E-3-phenyl-2-(1-phenylbenzimidazol-2-yl)acrylonitrile **3a**.

Compound **3a** was prepared from **1** (1.00 g, 4.33 mmol) and benzaldehyde **2a** (0.46 g, 4.33 mmol) in absolute ethanol (20 mL) and piperidine (0.15 mL) after heating under reflux for 3 h and recrystallization from ethanol to yield 0.90 g (65%) of yellow crystals; m.p. 136–138 °C; ^{1}H NMR (300 MHz, DMSO-d_6): δ = 7.91 (s, 1H, $H_{arom.}$), 7.88–7.38 (m, 2H, H_{arom}), 7.81 (d, 1H, J = 7.68 Hz, H_{arom}), 7.69–7.65 (m, 3H, H_{arom}), 7.64 (d, 2H, J = 1.84 Hz, H_{arom}), 7.56–7.52 (m, 3H, H_{arom}), 7.40–7.34 (m, 2H, H_{arom}), 7.23 (dd, 1H, J_1 = 7.60 Hz, J_2 = 1.83 Hz, H_{arom}); ^{13}C NMR (150 MHz, DMSO-d_6): δ = 150.9 (d), 147.1 (s), 142.4 (s), 137.3 (s), 135.6 (s), 132.9 (s), 132.5 (d), 130.7 (d, 2C), 130.0 (d, 3C), 129.7 (d, 2C), 127.9 (d, 2C), 124.9 (d), 123.9 (d), 120.1 (d), 116.0 (s), 111.1 (s), 101.1 (s); MS (*m*/*z*): 322 ($[M+1]^+$); UV (EtOH) λ_{max}: 337; Anal. Calcd for $C_{22}H_{15}N_3$ (321.1): C, 82.22; H, 4.70; N, 13.08. Found: C, 82.10; H, 4.62; N, 13.25.

2.2.2.2. E-3-(2-chlorophenyl)-2-(1-phenylbenzimidazol-2-yl)acrylonitrile **3b**.

Compound **3b** was prepared from **1** (0.69 g, 3.00 mmol) and 2-chlorobenzaldehyde **2b** (0.65 g, 3.00 mmol) in absolute ethanol (15 mL) and piperidine (0.10 mL) after heating under reflux for 3 h and recrystallization from ethanol to yield 0.49 g (77%) of yellow powder; m.p. 163–164 °C; ^{1}H NMR (600 MHz, DMSO-d_6): δ = 7.93 (d, 1H, J = 8.19 Hz, $H_{arom.}$), 7.85 (s, 1H, H_{arom}), 7.69 (d, 2H, J = 8.20 Hz, H_{arom}), 7.64–7.53 (m, 2H, H_{arom}), 7.46–7.40 (m, 4H, H_{arom}), 7.27 (d, 2H, J = 7.80 Hz, H_{arom}), 7.08 (d, 1H, J = 7.76 Hz, H_{arom}), 6.83 (d, 1H, J = 7.70 Hz, H_{arom}); ^{13}C NMR (150 MHz, DMSO-d_6): δ = 150.0 (d), 147.0 (s), 142.6 (s), 137.3 (s), 137.0 (s), 135.6 (s), 131.7 (d), 131.6 (d, 2C), 130.6 (d, 2C), 130.2 (s), 129.9 (d, 2C), 128.0 (d, 2C), 125.0 (d), 123.8 (d), 120.1 (d), 115.6 (s), 111.2 (s), 101.4 (s); MS (*m*/*z*): 356 ($[M+1]^+$); UV (EtOH) λ_{max}: 264; Anal. Calcd for $C_{22}H_{14}ClN_3$ (355.1): C, 74.26; H, 3.97; N, 11.81. Found: C, 74.14; H, 4.09; N, 11.66.

2.2.2.3. E-3-(4-chlorophenyl)-2-(1-phenylbenzimidazol-2-yl)acrylonitrile **3c**.

Compound **3c** was prepared from **1** (1.50 g, 6.50 mmol) and 4-chlorobenzaldehyde **2c** (1.42 g, 6.50 mmol) in absolute ethanol (20 mL) and piperidine (0.15 mL) after heating under reflux for 3.5 h and recrystallization from ethanol to yield 1.60 g (69%) of yellow crystals; m.p. 146–148 °C; ^{1}H NMR (600 MHz, DMSO-d_6): δ = 7.94 (s, 1H, $H_{arom.}$), 7.83 (d, 3H, J = 8.67 Hz, H_{arom}), 7.67–7.60 (m, 7H, $H_{arom.}$), 7.40–7.34 (m, 2H, $H_{arom.}$), 7.23 (dd, 1H, J_1 = 7.80 Hz, J_2 = 1.70 Hz, $H_{arom.}$); ^{13}C NMR (150 MHz, DMSO-d_6): δ = 149.5 (d), 146.9 (s), 142.4 (s), 137.4 (s), 137.0 (s), 135.5 (s), 131.7 (d), 131.5 (d, 2C), 130.7 (d, 2C), 130.0 (s), 129.8 (d, 2C), 128.0 (d, 2C), 124.9 (d), 123.7 (d), 120.2 (d), 115.7 (s), 111.2 (s), 101.7 (s); MS (*m*/*z*): 356 ($[M+1]^+$); UV (EtOH) λ_{max}: 344, 287; Anal. Calcd for $C_{22}H_{14}ClN_3$ (355.1): C, 74.26; H, 3.97; N, 11.81. Found: C, 74.12; H, 4.13; N, 11.69.

2.2.2.4. E-3-(4-nitrophenyl)-2-(1-phenylbenzimidazol-2-yl)acrylonitrile **3d**.

Compound **3d** was prepared from **1** (0.66 g, 2.86 mmol) and 4-nitrobenzaldehyde **2d** (0.43 g, 2.86 mmol) in absolute ethanol (15 mL) and piperidine (0.10 mL) after heating under reflux for 3.5 h and recrystallization from ethanol to yield 0.33 g (31%) of yellow crystals; m.p. 179–181 °C; ^{1}H NMR (600 MHz, DMSO-d_6): δ = 8.36 (d, 2H, J = 8.88 Hz, $H_{arom.}$), 8.08 (s, 1H, H_{arom}), 8,03 (d, 2H, J = 8.90 Hz, $H_{arom.}$), 7.85 (dd, 1H, J_1 = 7.98 Hz, J_2 = 2.10 Hz, $H_{arom.}$), 7.67–7.65 (m, 4H, $H_{arom.}$), 7.63–7.61 (m, 4H, $H_{arom.}$), 7.41–7.36 (m, 4H, $H_{arom.}$), 7.24 (d, 1H, J = 7.98 Hz); ^{13}C NMR (150 MHz, DMSO-d_6): δ = 146.9 (s), 143.7 (s), 141.7 (s), 133.7 (d), 132.3 (d), 131.4 (s), 131.3 (d), 130.5 (s), 129.5 (d), 126.7 (d), 125.6 (d), 125.3 (d), 124.2 (d), 123.6 (s), 123.4 (d), 120.4 (d), 115.6 (d), 115.0 (d), 114.5 (s); MS (*m*/*z*): 367

([M+1]$^+$); UV (EtOH) λ_{max}: 360, 276; Anal. Calcd for $C_{22}H_{14}N_4O_2$ (366.1): C, 72.12; H, 3.85; N, 15.29. Found: C, 72.30; H, 4.05; N, 14.98.

*2.2.2.5. E-3-(4-N,N-dimethylaminophenyl)-2-(1-phenylbenzimidazol-2-yl)acrylonitrile **3e**.* Compound **3e** was prepared from **1** (0.70 g, 3.03 mmol) and 4-*N*,*N*-dimethylamino- benzaldehyde **2e** (0.44 g, 3.03 mmol) in absolute ethanol (15 mL) and piperidine (0.15 mL) after heating under reflux for 3.5 h and recrystallization from ethanol to yield 0.26 g (21%) of orange crystals; m.p. 216–218 °C; ^{1}H NMR (600 MHz, DMSO-d_6): δ = 7.75 (d, 1H, J = 7.92 Hz, $H_{arom.}$), 7.70 (d, 2H, J = 9.06 Hz, H_{arom}), 7.69 (s, 1H, J = 5.64 Hz, $H_{arom.}$), 7.64 (t, 2H, J = 6.72 Hz, $H_{arom.}$), 7.61–7.57 (m, 3H, $H_{arom.}$), 7.32 (dt, 1H, J_1 = 7.53 Hz, J_2 = 1.15 Hz, $H_{arom.}$), 7.26 (dt, 1H, J_1 = 7.60 Hz, J_2 = 1.04 Hz, $H_{arom.}$), 7.15 (d, 1H, J = 7.87 Hz, $H_{arom.}$), 6.78 (d, 2H, J = 9.12 Hz, $H_{arom.}$), 3.03 (s, 6H, CH_3); ^{13}C NMR (150 MHz, DMSO-d_6): δ = 153.1 (s), 150.5 (d), 148.7 (s), 147.6 (s), 142.6 (s), 137.4 (s), 136.0 (s), 132.5 (d, 2C), 130.6 (d, 2C), 129.7 (d), 128.0 (d, 2C), 124.4 (d), 120.1 (d), 119.7 (d), 117.6 (s), 112.1 (d), 110.8 (d), 91.9 (s), 83.6 (s), 47.7 (q, 2C); MS (*m*/*z*): 365 ([M+1]$^+$); UV (EtOH) λ_{max}: 421; Anal. Calcd for $C_{24}H_{20}N_4$ (364.2): C, 79.10; H, 5.53; N, 15.37. Found: C, 79.30; H, 5.67; N, 15.60.

*2.2.3. E-3-(4-N,N-dimethylaminophenyl)-2-(1-phenylbenzimidazol-2-yl)acrylonitrile hydrochloride **3f***

A stirred suspension of compound **3e** (0.05 g, 0.10 mmol) in absolute ethanol (5 mL) was saturated with $HCl_{(g)}$. After 24 h of stirring at room temperature, the resulting product was filtered off and washed with diethylether (10 mL) to yield 0.04 g (73%) of red powder; m.p. >280 °C; ^{1}H NMR (600 MHz, DMSO-d_6): δ = ^{1}H NMR (DMSO-d_6) (δ/ppm) 7.88 (s, 1H, $H_{arom.}$), 7.78 (d, 1H, J = 8.10 Hz), 7.67–7.64 (m, 2H, $H_{arom.}$), 7.63–7.61 (m, 2H, $H_{arom.}$), 7.41 (dt, 1H, J_1 = 7.60 Hz, J_2 = 1.60 Hz, $H_{arom.}$), 7.35 (dt, 1H, J_1 = 7.75 Hz, J_2 = 1.80 Hz, $H_{arom.}$), 7.20 (d, 1H, J = 8.28 Hz, $H_{arom.}$), 6.80 (d, 2H, J = 9.10 Hz), 3.90 (brs, 1H, NH^+); ^{13}C NMR (150 MHz, DMSO-d_6): δ = 154.6 (s), 152.8 (d), 149.9 (s), 148.5 (s), 144.0 (s), 137.6 (s), 136.9 (s), 133.2 (d, 2C), 130.9 (d, 2C), 130.5 (d), 129.1 (d, 2C), 126.0 (d), 122.7 (s), 120.4 (d), 118.8 (d), 114.3 (d), 112.4 (d), 97.2 (s), 90.6 (s), 48.5 (q, 2C); MS (*m*/*z*): 365 ([M+1-HCl]$^+$); UV (EtOH) λ_{max}: 421; Anal. Calcd for $C_{24}H_{21}ClN_4$ (400.2): C, 71.90; H, 5.28; N, 13.98. Found: C, 71.75; H, 5.49; N, 13.75.

*2.2.4. General procedure for synthesis of compounds **4a**–**4d***

Ethanolic solutions of compounds **3a**–**3d** and small amount of iodine (5%), were irradiated at room temperature, with 400-W high-pressure mercury lamp, using a Pyrex filter for about 3–5 h, until the UV spectra shown that the reaction of dehydrocyclization was finished. Air was bubbled through the solution. The solutions were concentrated under reduced pressure and resulting product was separated by column chromatography on SiO_2 using dichlormethane as eluent.

*2.2.4.1. 5-Phenylbenzimidazo[1,2-a]quinoline-6-carbonitrile **4a**.* Compound **4a** was prepared from **3a** (0.30 g, 0.90 mmol) in ethanol (400 mL) after irradiation for 4 h and separation by column chromatography to yield 0.15 g (50%) of yellow powder; m.p. >280 °C; ^{1}H NMR (600 MHz, DMSO-d_6): δ = 8.95 (d, 1H, J = 8.46 Hz, $H_{arom.}$), 8.80 (d, 1H, J = 7.80 Hz, H_{arom}), 8.05–8.00 (m, 2H, $H_{arom.}$), 7.69–7.64 (m, 4H, $H_{arom.}$), 7.61–7.59 (m, 3H, $H_{arom.}$), 7.19–7.11 (m, 1H, $H_{arom.}$); ^{13}C NMR (150 MHz, DMSO-d_6): δ = 151.7 (s), 144.6 (s), 139.0 (s), 136.2 (s), 134.8 (s), 133.9 (d), 131.6 (s), 131.5 (d), 130.8 (d), 129.9 (d), 129.6 (d), 129.3 (d), 128.2 (d), 126.2 (s), 125.7 (d), 125.6 (d), 124.3 (d), 122.1 (s), 120.9 (d), 116.7 (d), 115.4 (d), 115.3 (s); MS (*m*/*z*): 320 ([M+1]$^+$); UV (EtOH) λ_{max}: 353, 265, 243; Anal. Calcd for $C_{22}H_{13}N_3$ (319.1): C, 82.74; H, 4.10; N, 13.16. Found: C, 82.89; H, 4.33; N, 13.40.

*2.2.4.2. 4-Chloro-5-phenylbenzimidazo[1,2-a]quinoline-6-carbonitrile **4b**.* Compound **4b** was prepared from **3b** (0.40 g, 1.10 mmol) in ethanol (400 mL) after irradiation for 4 h and separation by column chromatography to yield 0.19 g (48%) of yellow powder; m.p. >280 °C; ^{1}H NMR (600 MHz, DMSO-d_6): δ = 8.98 (d, 1H, J = 8.46 Hz, $H_{arom.}$), 8.82 (d, 1H, J = 8.40 Hz), 8.07 (dt, 1H, J_1 = 7.40 Hz, J_2 = 1.56 Hz, H_{arom}), 8.04 (dt, 1H, J_1 = 7.60 Hz, J_2 = 1.60 Hz, H_{arom}), 7.80 (d, 1H, J = 8.28 Hz, H_{arom}), 7.71–7.67 (m, 2H, H_{arom}), 7.67–7.61 (m, 2H, H_{arom}), 7.59 (dd, 1H, J_1 = 7.90 Hz, J_2 = 1.60 Hz, H_{arom}), 7.59 (d, 1H, J = 7.90 Hz, H_{arom}), 7.37 (dd, 1H, J_1 = 8.10 Hz, J_2 = 1.77 Hz); ^{13}C NMR (150 MHz, DMSO-d_6): 151.2 (s), 147.6 (s), 145.0 (s), 136.0 (s), 135.5 (s), 134.3 (s), 134.0 (d), 132.0 (d), 131.3 (s), 130.1 (d, 2C), 128.7 (d), 128.6 (d), 125.6 (d, 2C), 124.4 (d), 121.7 (s), 120.9 (d), 116.9 (d), 115.4 (s), 115.3 (d), 102.5 (s); MS (*m*/*z*): 354 ([M+1]$^+$); UV (EtOH) λ_{max}: 255, 265; Anal. Calcd for $C_{22}H_{12}ClN_3$ (353.1): C, 74.68; H, 3.42; N, 11.88. Found: C, 74.85; H, 3.20; N, 11.60.

*2.2.4.3. 2-Chloro-5-phenylbenzimidazo[1,2-a]quinoline-6-carbonitrile **4c**.* Compound **4c** was prepared from **3c** (0.40 g, 1.10 mmol) in ethanol (400 mL) after irradiation for 5 h and separation by column chromatography to yield 0.18 g (45%) of yellow powder; m.p. >280 °C; ^{1}H NMR (600 MHz, DMSO-d_6): δ = 8.96 (d, 2H, J = 8.49 Hz, $H_{arom.}$), 8.81 (dd, 1H, J_1 = 8.50 Hz, J_2 = 1.78 Hz), 8.08–8.00 (m, 2H, $H_{arom.}$), 7.74 (d, 2H, J = 8.34 Hz, $H_{arom.}$), 7.63–7.61 (m, 2H, $H_{arom.}$), 7.59–7.56 (m, 3H, $H_{arom.}$); ^{13}C NMR (150 MHz, DMSO-d_6): 150.5 (s), 148.0 (s), 144.5 (s), 136.1(s), 135.2 (s), 134.1 (d), 133.6 (s), 131.9 (d), 131.0 (s), 130.2 (d, 2C), 129.1 (d, 2C), 127.6 (d), 125.5 (d), 124.3 (d), 121.9 (s), 120.8 (d), 116.8 (d), 115.4 (d), 115.3 (s), 102.4 (s); MS (*m*/*z*): 354 ([M+1]$^+$); UV (EtOH) λ_{max}: 355, 266, 254; Anal. Calcd for $C_{22}H_{12}ClN_3$ (353.1): C, 74.68; H, 3.42; N, 11.88. Found: C, 74.89; H, 3.25; N, 11.65.

*2.2.4.4. 2-Nitro-5-phenylbenzimidazo[1,2-a]quinoline-6-carbonitrile **4d**.* Compound **4d** was prepared from **3d** (0.30 g, 0.80 mmol) in ethanol (400 mL) after irradiation for 3 h and separation by column chromatography to yield 0.18 g (60%) of yellow powder; m.p. >280 °C; ^{1}H NMR (600 MHz, DMSO-d_6): δ = 9.00 (d, 1H, J = 8.52 Hz, H_{arom}), 8.79 (d, 1H, J = 7.74 Hz, H_{arom}), 8.42 (d, 1H, J = 8.76 Hz, H_{arom}), 8.41 (d, 1H, J = 8.52 Hz, H_{arom}), 8.16–8.05 (m, 2H, H_{arom}), 7.98 (d, 1H, J = 8.88 Hz, H_{arom}), 7.78 (d, 2H, J = 8.98 Hz, H_{arom}), 7.64–7.57 (m, 2H, H_{arom}), 7.37 (d, 1H, J = 8.64 Hz, H_{arom}); ^{13}C NMR (150 MHz, DMSO-d_6): δ = 149.0 (s), 146.9 (s), 143.7 (s), 141.6 (s), 135.6 (s), 133.7 (d), 132.3 (d, 2C), 131.6 (s), 131.4 (d), 129.0 (d), 126.7 (d), 125.4 (d), 124.6 (d), 123.6 (s), 123.2 (d, 2C), 121.1 (s), 120.4 (d), 117.3 (s), 115.6 (d), 114.5 (s); MS (*m*/*z*): 365 ([M+1]$^+$); UV (EtOH) λ_{max}: 264; Anal. Calcd for $C_{22}H_{12}N_4O_2$ (364.1): C, 72.52; H, 3.32; N, 15.38. Found: C, 72.77; H, 3.11; N, 15.55.

*2.2.5. 2-Amino-5-phenylbenzimidazo[1,2-a]quinoline-6-carbonitrile **5***

Compound **4d** (0.11 g, 0.30 mmol) and solution of $SnCl_2 \times 2H_2O$ (0.54 g, 2.4 mmol) in MeOH (0.9 mL) and concentrated HCl (0.9 mL) were heated under reflux for 0.5 h. After cooling, the reaction mixture was evaporated under vacuum and dissolved in water (20 mL). The resulting solution was treated with 20% NaOH to pH = 14. Resulting product was filtered off and washed with water to yield 0.03 (69%) of yellow powder; m.p. >280 °C; ^{1}H NMR (600 MHz, DMSO-d_6): δ = 8.92 (d, 1H, J = 8.70 Hz, H_{arom}), 8.03 (dd, 2H, J_1 = 8.98 Hz, J_2 = 1.78 Hz, H_{arom}), 7.83 (dd, 2H, J_1 = 8.70 Hz, J_2 = 1.38 Hz, H_{arom}), 7.64–7.51 (m, 2H, H_{arom}), 7.39 (d, 1H, J = 8.76 Hz, H_{arom}), 7.30 (d, 1H, J = 8.80 Hz, H_{arom}), 7.07 (d, 2H, J = 8.37 Hz, H_{arom}), 6.71 (d, 1H, J = 8.34 Hz, H_{arom}), 5.70 (brs, 2H, NH_2); ^{13}C NMR (150 MHz, DMSO-d_6): δ = 149.6 (s), 147.2 (s), 144.1 (s), 142.0 (s), 135.5 (s), 134.1 (d), 133.1 (d, 2C), 131.9 (d), 131.7 (s), 129.4 (d), 127.1 (d), 125.6 (d), 124.8 (d), 124.4 (s), 123.7 (d, 2C), 121.8 (s), 120.9 (d), 118.0 (s), 116.1 (d), 115.0 (s); MS (*m*/*z*): 335 ([M+1]$^+$); UV (EtOH) λ_{max}: 360, 344, 260; Anal. Calcd for $C_{22}H_{14}N_4$ (334.1): C, 79.02; H, 4.22; N, 16.76. Found: C, 79.32; H, 4.13; N, 16.55.

2.2.6. 2-Amino-5-phenylbenzimidazo[1,2-a]quinoline-6-carbonitrile hydrochloride **6**

A stirred suspension of compound **5** (0.03 g, 0.09 mmol) in absolute ethanol (5 mL) was saturated with $HCl_{(g)}$. After 24 h of stirring at room temperature, the resulting product was filtered off and washed with diethylether (5 mL) to yield 0.02 g (61%) of yellow powder; m.p. >280 °C; ^{1}H NMR (600 MHz, DMSO-d_6): δ = 8.00 (d, 1H, J = 8.68 Hz, H_{arom}), 7.78 (d, 1H, J = 7.98 Hz, H_{arom}), 7.75 (d, 1H, J = 8.70 Hz, H_{arom}), 7.67–7.63 (m, 3H, H_{arom}), 7.41 (dt, 1H, J_1 = 7.98 Hz, J_2 = 1.02 Hz, H_{arom}), 7.35 (dt, 2H, J_1 = 7.98 Hz, J_2 = 1.02 Hz, H_{arom}), 7.19 (dd, 1H, J_1 = 8.10 Hz, J_2 = 1.40 Hz, H_{arom}), 6.80 (d, 2H, J = 8.80 Hz, H_{arom}), 4,80 (brs, 3H, NH_3^+); ^{13}C NMR (150 MHz, DMSO-d_6): δ = 149.3 (s), 147.0 (s), 144.5 (s), 142.6 (s), 135.6 (s), 134.4 (d), 133.3 (d, 2C), 132.2 (d), 131.9 (s), 129.3 (d), 126.2 (d), 125.4 (d), 124.6 (d), 124.6 (s), 123.8 (d, 2C), 121.9 (d), 121.7 (s), 118.4 (s), 116.3 (d), 114.7 (s); MS (m/z): 335 ([M+1-HCl]$^+$); UV (EtOH) λ_{max}: 361, 345, 264; $C_{22}H_{15}ClN_4$ (370.1): C, 71.25; H, 4.08; N, 15.11. Found: C, 71.40; H, 4.33; N, 14.87.

2.3. Spectroscopic characterization

UV absorption spectra were recorded, against the solvent, at (25 ± 0.1) °C, using a Varian Cary 50 spectrophotometer operated in double-beam mode. The wavelength range covered was 200–450 nm. Quartz cells of 1-cm path length were used throughout and absorbance values were recorded at 0.1 nm. Fluorescence measurements were carried out on a Varian Cary Eclipse fluorescence spectrophotometer at 25 °C using 1-cm path quartz cells. Excitation maxima were determined from excitation spectra covering the range of 200–450 nm. Emission spectra were recorded from 400 to 600 nm and corrected for the effects of time- and wavelength-dependent light-source fluctuations using a standard of rhodamine 101, a diffuser provided with the fluorimeter and the software supplied with the instrument. The measurements were performed in ethanol (HPLC grade). Relative fluorescence quantum yields were determined according to *Miller* using Eq. (1):

$$\phi_X = \phi_S \times A_S D_X n_X^2 / A_X D_S n_S^2$$

where in ϕ is the emission quantum yield, A is the absorbance at the excitation wavelength, D is the area under the corrected emission curve and n is the refractive index of the solvents used. The subscripts s and x refer to the standard and to the unknown, respectively. The standard employed was quinine sulfate with a published fluorescence quantum yield of 0.54 [28]. All samples were purged with argon to displace oxygen. The reproducibility (difference between the largest and the smallest value in a series of three independent measurements, divided by their arithmetic mean) of quantum yield measurements was better than 10%.

2.4. Single-crystal X-ray diffraction experiment

Selected crystallographic and refinement data for structures **3d** and **4a** obtained by the single-crystal X-ray diffraction experiment are reported in Table 1. Tables 2 and 3 contain selected molecular geometry parameters for structures **3d** and **4a**, respectively. Table 4 lists hydrogen bond and interaction geometry for **3d** and **4a**, while Table 5 contains geometry of π···π interactions.

Data collection for both structures **3d** and **4a**, has been performed by applying the CrysAlis Software system, Version 1.171.34.40 [29]. The Lorentz-polarization effect was corrected and the intensity data reduced by the CrysAlis RED application of the CrysAlis Software system, Version 1.171.34.40 [29]. The diffraction data have been scaled for absorption effects by the multi-scanning method.

Table 1
General and crystal data and summary of intensity data collection and structure refinement for compounds **3d** and **4a**.

	3d	**4a**
Formula	$C_{22}H_{14}N_4O_2$	$C_{22}H_{13}N_3$
M_r	366.37	319.35
Crystal system, colour and habit	Monoclinic, yellow prism	Monoclinic, yellow prism
Space group	$P\,2_1/n$	$P\,2_1/c$
Crystal dimensions (mm^3)	0.42 × 0.18 × 0.15	0.38 × 0.22 × 0.16
Unit cell parameters:		
a (Å)	5.4466(7)	9.6785(2)
b (Å)	26.373(3)	16.3577(4)
c (Å)	12.6600(16)	10.4937(2)
β/°	101.244(13)	103.910(2)
V (Å^3)	1783.6(4)	1612.62(6)
Z	4	4
D_c (g cm^{-3})	1.364	1.315
μ (mm^{-1})	0.091	0.621
F(000)	760	664
θ range for data collection (°)[a]	4 to 25	5 to 73
h,k,l range	−6 to 3, −30 to 31, −15to 14	−8 to 11, −17 to 20, −12 to 12
Scan type	ω	ω
No. measured reflections	6843	7806
No. independent reflections ($R_{int.}$)	3125 (0.0898)	3169 (0.036)
Data/restraints/parameters	3125/0/254	3169/0/226
No. observed reflections, $I \geq 2\sigma(I)$	1481	2456
Completeness (%)	99.4 (to θ = 25.00°)	99.3(to θ = 72.5°)
g_1, g_2 in w	0.0314, 0.000	0.0798, 0.1647
R, wR [$I \geq 2\sigma(I)$]	0.0505, 0.0709	0.0458, 0.1225
R, wR [all data]	0.1573, 0.0864	0.0614, 0.1492
Goodness of fit on F^2, S	0.869	1.053
Extinction coefficient	0.0101(9)	–
Min. and max. electron density (e Å^{-3})	−0.135, 0.134	−0.195, 0.145
Maximum Δ/σ	<0.001	0.001

[a] The data collection for compound **3d** were collected by ω-scans on an Oxford Xcalibur diffractometer equipped with 4-circle kappa geometry and CCD Sapphire 3 detector and graphite-monochromated Mo$K\alpha$ radiation (λ = 0.71073 Å) at ambient temperature (296 K) and for compound **4a** on an Oxford Xcalibur diffractometer equipped with 4-circle kappa geometry and CCD Ruby detector and graphite-monochromated Cu$K\alpha$ radiation (λ = 1.5418 Å) at ambient temperature (296 K).

Structures were solved by direct methods and refined on F^2 by weighted full-matrix least-squares. Programs SHELXS97 [30] and SHELXL97 [30] integrated in the WinGX (v. 1.70.01) [31] software system were used to solve and refine structure. All non-hydrogen atoms were refined anisotropically. Hydrogen atoms belonging to Csp^2 carbon atoms were placed in geometrically idealized positions [Csp^2-H 0.93 Å with $U_{iso}(H) = 1.2\,U_{eq}(C)$] and they were constrained to ride on their parent atoms by using the appropriate SHELXL97 HFIX instructions. The molecular geometry calculations were done using PLATON [32] and PARST [33] programs. Graphics were done using ORTEP-3 [34] and PovRay [35] and Mercury [36]. All programs are integrated in the WinGX software system [31].

3. Results and disscussion

3.1. Synthesis

All newly prepared compounds presented in Fig. 1. were synthesized according to the two synthetic procedures shown in Scheme 1 and Scheme 2.

Acyclic compounds **3a**–**3f** were prepared by conventional methods for the preparation of similar benzimidazole derivatives,

Table 2
Electronic absorption and fluorescence emission data of studied compounds in ethanol.

Comp.	**3a**	**3c**	**3d**	**3e**	**3f**	**4a**	**4b**	**4c**	**4d**	**5**
λ_{max}/nm	332	339	361	408	476	353	354	356	361	363
	277	281	278	241		268	263	265	245	343
		230	205			244	241	244	261	266
		205				209				
$\varepsilon \times 10^3$	30.05	13.55	17.50	27.60	46.50	7.10	11.15	16.35	9.20	9.50
($dm^3\ mol^{-1}\ cm^{-1}$)	23.05	10.00	13.65	11.80		22.80	27.00	44.20	8.85	8.80
		16.60	49.40			19.00	28.85	38.45	29.25	33.00
		37.70				25.95				
λ_{emiss}/nm	478	481	561	431	489	483	478	485	478	460
Rel. Fluo. Int. (arb. un.)	63.9	78.1	128.1	204.1	58.0	629.5	491.9	307.1	32.1	23.6
ϕ	<0.01	<0.01	<0.01	<0.01	<0.01	0.40	0.53	0.58	0.05	0.06
Stokes shift (nm)	146	142	200	23	13	130	124	94	117	97

Table 3
Selected interatomic distances (Å) and valence and torsion angles (°) for the compound **3d**.

3d	
Selected bond distances	
C1–N1	1.383(3)
C1–N2	1.311(3)
C1–C8	1.472(3)
C8–C9	1.346(3)
C8–C16	1.424(4)
C9–C10	1.465(3)
Selected bond angles	
C9–C8–C16	122.9(2)
C9–C8–C1	119.4(2)
C16–C8–C1	117.6(2)
C8–C9–C10	130.7(2)
Selected torsion angle	
C18–C17–N1–C7	105.7(3)

in a cyclocondensation starting from the 2-cyanomethyl-*N*-phenylbenzimidazole **1** and the corresponding aromatic benzaldehydes **2a**–**2d**. Cyclic benzimidazo[1,2-*a*]quinolines **4a**–**4d** were prepared by photochemical dehydrocyclization of an ethanolic solution of compounds **3a**–**3d** after separation on chromatography silica gel. All photochemical reactions were followed by UV/Vis spectroscopy. Amino substituted compound **5** was prepared from nitro substituted compound **4d** by reduction with $SnCl_2 \times 2H_2O$ in MeOH and concentrated HCl. The hydrochloride salts **3f** and **6** of *N,N*-dimethylamino **3e** and amino **5** substituted compounds were prepared with HCl_{gas}. All structures of novel *E*-3substituted-2-(1-phenylbenzimidazol-2-yl)acrylonitriles **3a**–**3e** and 2,4-substituted-5-phenyl-benzimidazo[1,2-*a*]quinoline-6-carbonitriles **4a**–**4d** and **5**–**6** were determined by the NMR analysis based on the analysis of H–H coupling constants as well as chemical shifts and by mass spectroscopy. The photocyclization reaction leads to a downfield shift of the signal of most aromatic protons in their ^{1}H NMR along with disappearance of one aromatic proton on the acrylonitrile part of the molecule. Migration of a phenyl ring from benzimidazole to acrylonitrile part of cyclic skeleton was additionally confirmed with 2D NMR spectroscopy based on NOE interactions of specific aromatic signals. ^{1}H NMR spectra of the amino substituted benzimidazo[1,2-*a*]quinoline **5** showed appearance of broad singlet which belong to two protons of amino group. ^{1}H NMR spectra of amino substituted benzimidazo[1,2-*a*]quinoline hydrochloride **6** showed a downfield shift of most of the signals in comparison with ^{1}H NMR spectra of compound **5**.

Table 4
Selected interatomic distances (Å) and valence and torsion angles (°) for the compound **4a**.

4a	
Selected bond distances	
N1–C1	1.312(2)
N1–C15	1.383(2)
N2–C1	1.3880(19)
N2–C9	1.3999(19)
N2–C10	1.4011(18)
C3–C16	1.491(2)
Selected torsion angle	
C2–C3–C16–C17	90.9(2)

3.2. Spectroscopic characterization

In order to study the spectroscopic properties of prepared compounds **3a, 3c, 3d, 3e, 3f, 4a, 4c, 4d** and **5**, UV/Vis and fluorescence emission spectra were recorded in ethanol. The stock solutions of compounds were prepared in ethanol by concentrations as it follows: c(**3a**) = 4.05 × 10^{-3} mol dm^{-3}; c(**3c**) = 5.06 × 10^{-4} mol dm^{-3}; c(**3d**) = 3.55 × 10^{-3} mol dm^{-3}; c(**3e**) = 1,24 × 10^{-5} mol dm^{-3}; c(**3f**) = 1.37 × 10^{-3} mol dm^{-3}; c(**4a**) = 6.8 × 10^{-4} mol dm^{-3}; c(**4b**) = 2.0 × 10^{-4} mol dm^{-3}; c(**4c**) = 3.9 × 10^{-4} mol dm^{-3}; c(**4d**) = 2.7 × 10^{-4} mol dm^{-3}; c(**5**) = 5.1 × 10^{-4} mol dm^{-3}. UV/Vis spectra of prepared compounds were recorded at the same concentration of 2.0 × 10^{-5} mol dm^{-3} and can be visualized in Fig. 2.

Acyclic compounds **3a** and **3c** showed one intense main absorption band at 332 and 339 nm, nitro substituted compound **3d** at 361 nm while *N,N*-dimethylamino substituted compounds **3e** and **3f** showed intense bathochromic shift of ~90 nm relative to **3a** and **3c** and absorption maxima at 422 and 425 nm, respectively. Heteroatoms, such as nitrogen, with non-bonding electrons which can take part in the resonance and cause a bathochromic shift, can absorb UV radiation when the electrons make a transition from *n*

Table 5
Hydrogen bond and weak interaction geometry (Å, °) for compounds **3d** and **4a**.

D–H···A	D–H	H···A	D···A	∠D–H···A	Symmetry code
3d					
C9–H9···O1	0.93	2.57	3.477(3)	165	−1/2 + *x*,1/2−*y*,1/2 + *z*
C18–H18···N3	0.93	2.68	3.554(3)	157	*x* + 1,+*y*,+*z*
4a					
C8–H8···N3	0.93	2.48	3.243(2)	139	1 + *x*,*y*,*z*
C11–H11···N3	0.93	2.73	3.655(2)	173	1 + *x*,*y*,*z*

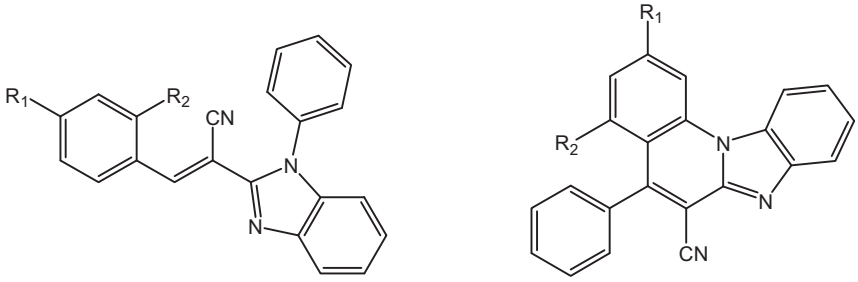

3a R_1=H, R_2=H
3b R_1=H, R_2=Cl
3c R_1=Cl, R_2=H
3d R_1=NO_2, R_2=H
3e R_1=$N(CH_3)_2$, R_2=H
3f R_1=$N(CH_3)_2$×HCl, R_2=H

4a R_1=H, R_2=H
4b R_1=H, R_2=Cl
4c R_1=Cl, R_2=H
4d R_1=NO_2, R_2=H
5 R_1=NH_2, R_2=H
6 R_1=NH_2×HCl, R_2=H

Fig. 1. Synthesized acyclic benzimidazole derivatives **3a**–**3f** and cyclic benzimidazo[1,2-*a*]quinolines **4a**–**4d**, **5** and **6**.

orbitals to π* orbitals. Cyclic compounds **4a, 4c, 4d** and **5** display several absorption bands (Table 2), especially intense in the region from 240 to 275 nm with high extinction coefficients. Most of these electronic transitions are made from π to π* orbital of the tetracyclic conjugated π-system. Conversion of nitro into the amino substituent did not resulted in changes in absorbance spectra while introduction of a chlorine substituent resulted in a hypechromic shift of the absorbance intensity and an increasing in the molar extinction coefficients.

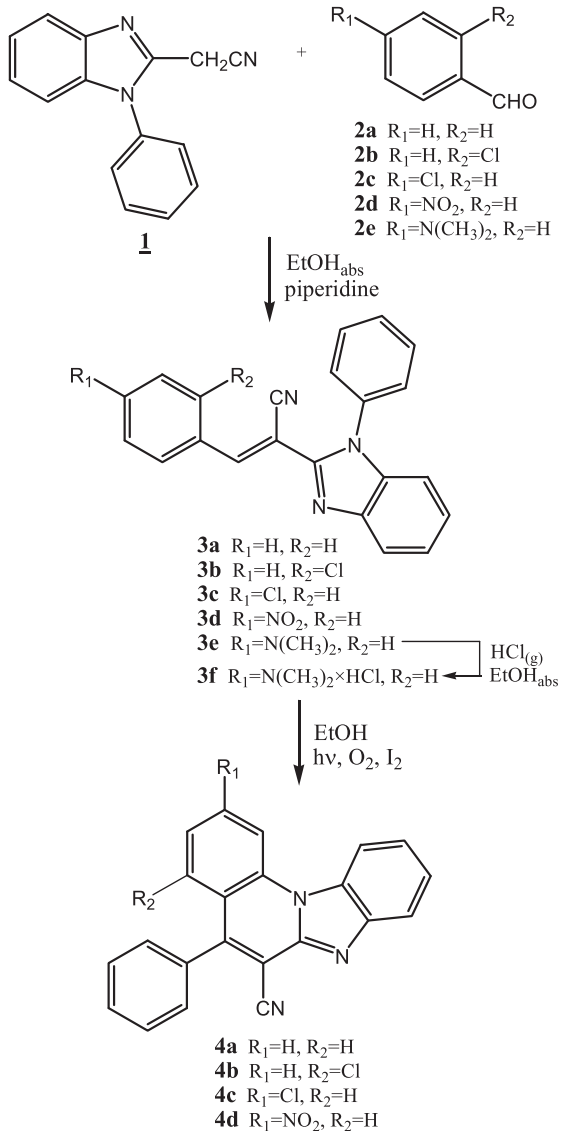

2a R_1=H, R_2=H
2b R_1=H, R_2=Cl
2c R_1=Cl, R_2=H
2d R_1=NO_2, R_2=H
2e R_1=$N(CH_3)_2$, R_2=H

1

$EtOH_{abs}$
piperidine

3a R_1=H, R_2=H
3b R_1=H, R_2=Cl
3c R_1=Cl, R_2=H
3d R_1=NO_2, R_2=H
3e R_1=$N(CH_3)_2$, R_2=H
3f R_1=$N(CH_3)_2$×HCl, R_2=H

$HCl_{(g)}$
$EtOH_{abs}$

EtOH
hν, O_2, I_2

4a R_1=H, R_2=H
4b R_1=H, R_2=Cl
4c R_1=Cl, R_2=H
4d R_1=NO_2, R_2=H

Scheme 1. Synthesis of compounds **3a**–**3f** and **4a**–**4d**.

Fluorescence emission spectra were recorded at the same concentration of 2.0×10^{-6} mol dm^{-3} for acyclic compounds **3a, 3c, 3d, 3e** and **3f,** and 5.0×10^{-7} mol dm^{-3} for cyclic compounds **4a, 4b, 4c, 4d** and **5** and can be visualized in Fig. 3.

Fluorescence excitation was performed at the wavelength of maximum absorption. All compounds exhibit characteristic fluorescence emission with a single emission band. Nitro substituted acyclic compound **3d** showed an intense batochromic shift with emission maxima at 561 nm, *N,N*-dimethylamino substituted compound **3e** showed one emission maxima at 431 nm while other acyclic compounds showed low fluorescence intensity and emission maxima at ~480 nm. Cyclic compounds also showed a single emission band (Table 2). Compound **4a** showed the highest fluorescence intensity amongst all studied compounds. Additional substituents did not yield any significant change of emission maxima and have caused only hyperchromic shift of fluorescence intensity. Electronic absorption and fluorescence data of studied compounds recorded at the same concentration in ethanol, quantum yield data φ and Stokes shift values are summarized in Table 2.

Excitation spectra of all studied compounds are in a good agreement with their absorption spectra. The difference in energy between the absorbed and emitted radiation is known as the Stokes shift. All compounds except **3e** and **3f** possessed large Stokes shift values (94–200 nm) which could be generally attributed to a different charge distribution (or geometry) in the excited state of molecules compared to the ground state.

3.3. Crystal structure analysis of compounds *3d* and *4a*

3.3.1. Crystal structure description of compound *E*-3-(4-nitrophenyl)-2-(1-phenyl benzimidazol-2-yl)-acrylonitrile *3d*

ORTEP-POV-Ray rendered view of the molecular structure of **3d** is depicted in Fig. 4.

The molecule deviates from planarity in the solid state which is described by the dihedral angle [18.6(1)°] calculated between best planes through the atoms of the phenyl (C10 − C15) and benzimidazole ring (C1, N1, N2, C2, C3, C4, C5, C6 and C7). We recently published analogous structures belonging to the class of 2-benzimidazolyl substituted acrylonitriles such as monohydrates

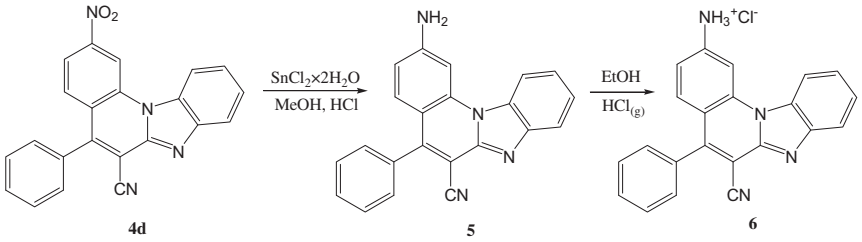

Scheme 2. Synthesis of compounds **5** and **6**.

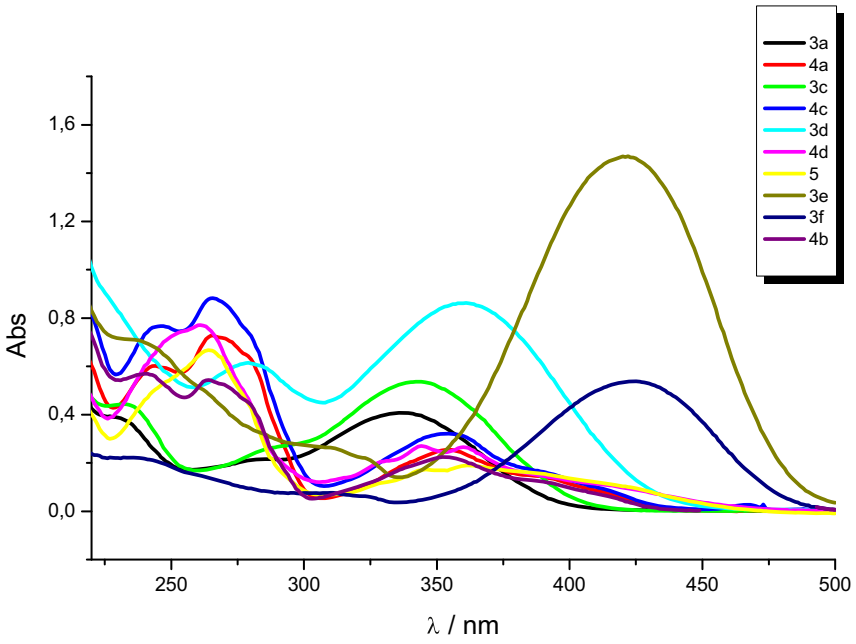

Fig. 2. UV/Vis spectra of compounds **3a, 3c, 3d, 3e, 3f, 4a, 4c, 4d** and **5** in ethanol.

of 2-(1*H*-benzimidazol-2-yl)-3-(4-cyanophenyl)-acrylonitrile and 2-(1*H*-benzimidazol-2-yl)-3-(4-bromophenyl)-acrylonitrile [36] which do not deviate significantly from planarity [5.6(1)o and 3.5(1)°, respectively] and 2-(2-benzimidazolyl)-3-(4-fluorophenyl) acrylonitrile ethanol solvate which molecules deviate from planarity by 13.11(2)° [27]. All three above-mentioned 2-

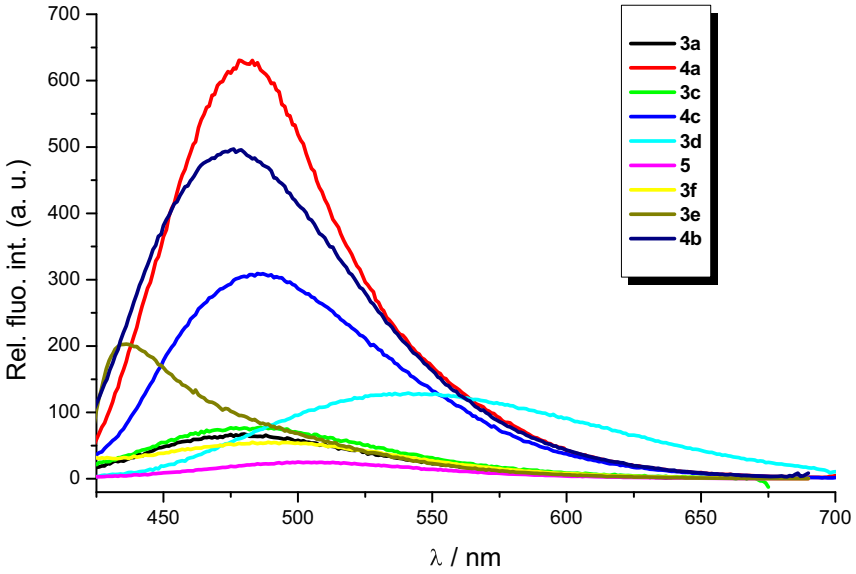

Fig. 3. Fluorescence emission spectra of compounds **3a, 3c, 3d, 3e, 3f, 4a, 4b, 4c, 4d** and **5** in ethanol.

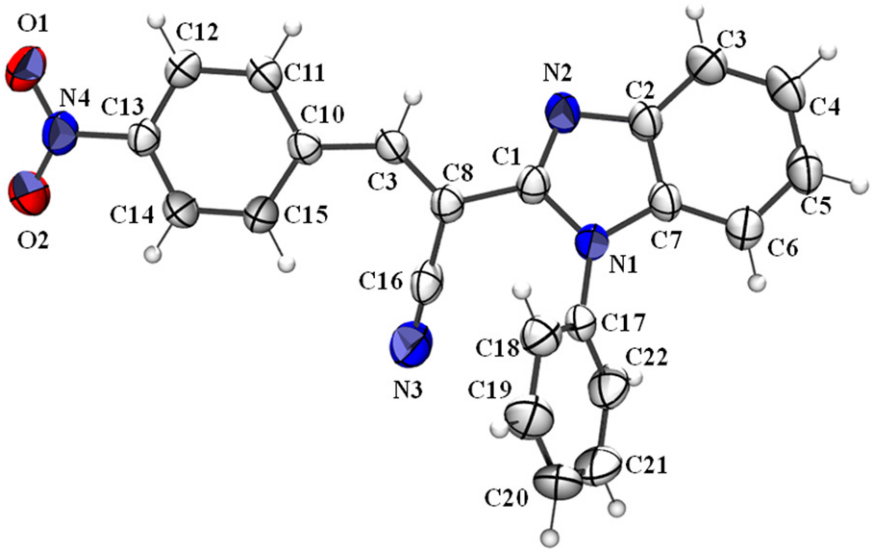

Fig. 4. ORTEP-POV-Ray rendered view of the asymmetric unit of **3d** with atom labeling schemes. The displacement ellipsoids are drawn at the 50% probability level at 296(2) K.

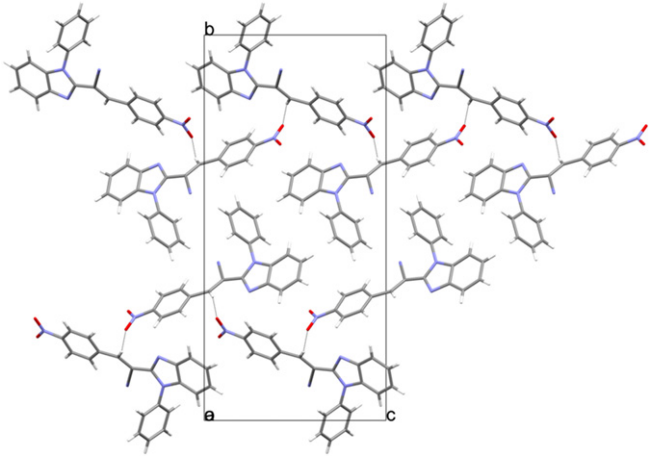

Fig. 5. Crystal packing of **3d** viewed down *a* axis. Dashed lines represent C–H···O intermolecular hydrogen bond linking molecules into infinite *zig-zag* chains spreading along *c* axis.

benzimidazolyl substituted acrylonitrile derivatives are differently functionalized at position 4 of phenyl ring: by cyano group, bromine atom, fluorine atom and nitro group in the case of compound **3d**. Compound **3d** is additionally substituted by phenyl group at the N1 atom of 2-benzimidazolyl moiety, while in the previously published structures this is not the case. The spatial orientation of phenyl ring in respect to the plane of benzimidazole ring is given by the dihedral angle value of 67.2(1)°. The bond distances C1–C8 and C9–C10 are predominantly σ in character showing delocalization effect to a larger extent (1.472(3) Å and 1.465(3) Å, respectively). The C8 = C9 bond is dominantly π in character (1.346(3) Å; Table 3). The value of C8-C16 bond distance (1.424(4) Å) is influenced by the presence of the nearby cyano group. Since the groups attached to C8 and C9 with the higher priority lie on the same side of a plane containing the double C8 = C9 bond, the stereoisomer **3d** in the crystalline state is designated as *E*.

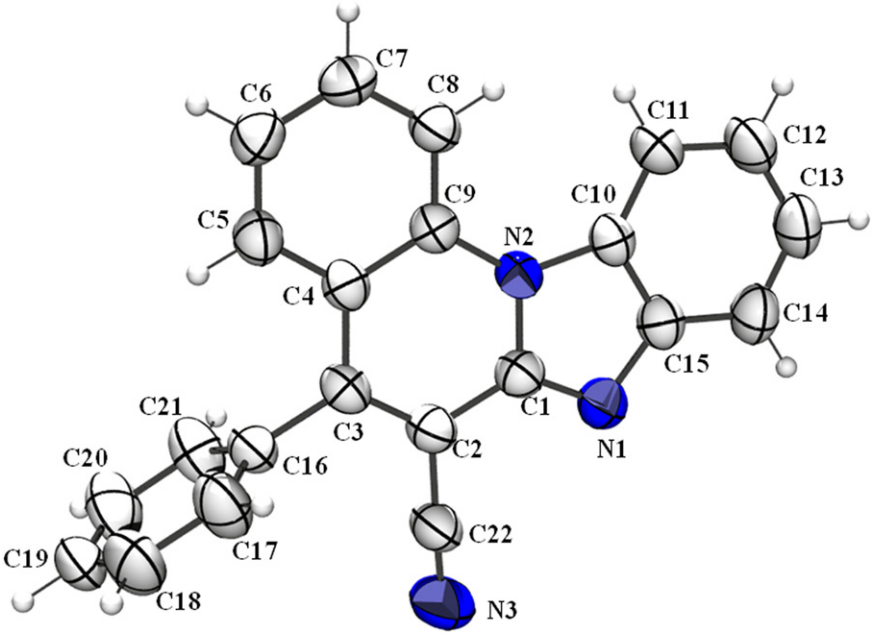

Fig. 6. ORTEP-POV-Ray rendered view of the asymmetric unit of **4a** with atom labeling schemes. The displacement ellipsoids are drawn at the 50% probability level at 296(2) K.

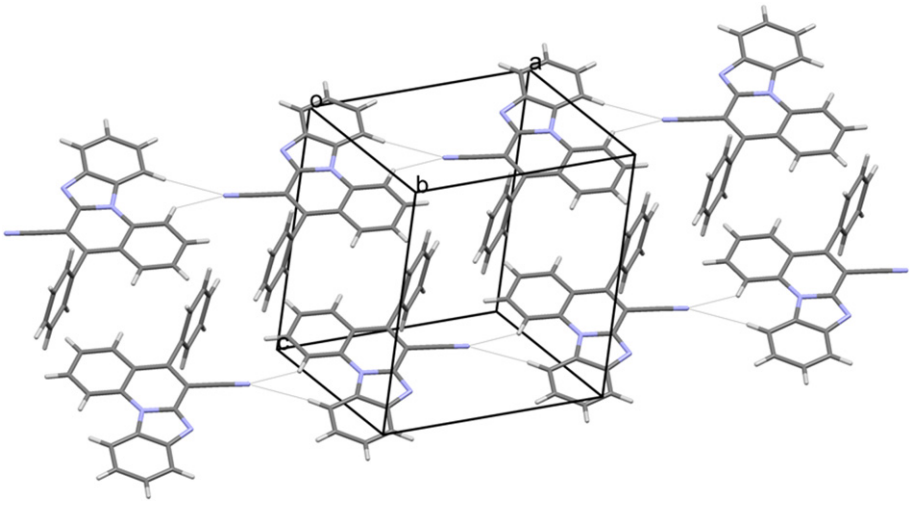

Fig. 7. Crystal packing of **4a** showing antiparallel layers of chains formed by C–H···Nhydrogen bonds (in dashed lines). The chains are spreading along *a* axis.

The crystal structure is dominated by the C9–H9···O1 (Table 4) intermolecular hydrogen bond between –CH proton donor group and the oxygen atom from nitro group linking molecules into infinite *zig-zag* chains spreading along the *c* axis (Fig. 5).

The very weak C–H···N interaction including one of the aryl –CH group and the cyano nitrogen atom N3 as a proton acceptor is also present (Table 4). No π···π interactions are found.

3.3.2. *Crystal structure description of compound 5-phenyl-benzimidazo [1,2-a]quinoline-6-carbonitrile **4a***

ORTEP-POV-Ray rendered view of the molecular structure of **3d** is depicted in Fig. 6.

We have recently published the crystal and molecular structures of the six compounds which belong to the class of benzimidazo[1,2-*a*]quinoline-6-carbonitriles functionalized at position 2 by: bromine atom in the structure of 2-bromo-benzimidazo[1,2-*a*]quinoline-6-carbonitrile [37], cyano group in the structure of benzimidazo[1,2-*a*]quinoline-2,6-dicarbonitrile [37], methyl group in 2-methylbenzimidazo[1,2-*a*]quinoline-6-carbonitrile [27], fluorine atom in 2-fluoro-benzimidazo[1,2-*a*]quinoline-6-carbonitrile [27], chlorine atom in 2-chlorobenzimidazo[1,2-*a*]quinoline-6-carbonitrile [28] and by piperidine in 2-piperidinylbenzimidazo [1,2-*a*]quinoline-6-carbonitrile [28]. The compound **4a** is additionally substituted at position 5 by the phenyl ring which does not lie in the plane defined by essentially planar benzimidazo[1,2-*a*] quinoline-6-carbonitrile structural fragment (dihedral angle calculated between two best planes amounts 89.0(1)°). The benzimidazo[1,2-*a*]quinoline fragment contains an sp^3 hybridized N2 atom, the lone pair electrons of which are delocalized within the π-system of fused rings. The C–N bond distances with the sp^3 hybridized N2 atom (C1-N2, C9-N2 and C10-N2) are significantly longer than C–N bonds formed by the sp^2 hybridized N1 atom (shorter C1-N1 and longer C15-N1 in imidazolyl ring), which are dominantly π in character (Table 4), as it is found in analogous benzimidazo[1,2-*a*]quinolines [27,28,37]. The compound **4a** does not contain strong proton donors, therefore the molecular assembly within crystal structure is characterized by the existence of the weak C–H···N hydrogen bonds formed between phenyl –CH groups and the N3 atom of the cyano group (Table 5, Fig. 7). The N3 atom acts as a double proton acceptor forming stronger and weaker C–H···N hydrogen bond linking molecules into infinite chains along the *a* axis. The chains spread into layers along the *c* axis interacting mutually through π···π interactions (Table 6).

Table 6
Geometrical parameters of π···π interactions[a] (Å, °) for compound **4a**.

Interaction[b]	C_g–C_g distance	C_g···P1[b,c]	C_g···P2[d]	α[e]	β[f]	Slippage
4a						
Cg1···Cg3	3.7696(9)	3.3021(7)	3.3982(7)	3.22(8)	25.65	1.632
Cg3···Cg1	3.7696(9)	3.3983(7)	3.3021(7)	3.22(8)	28.84	1.818
Cg3···Cg4	3.766(1)	3.4207(7)	3.4196(7)	4.84(8)	24.75	1.576
Cg4···Cg3	3.766(1)	3.4196(7)	3.4207(7)	4.84(8)	24.71	1.576

[a] Those possible interactions for which perpendicular distance between two planes is longer than 3.8 Å (3.3–3.8 Å) (C_g···P1 and C_g···P2; the perpendicular distance of corresponding centroid to a plane) and dihedral angles (between P1 and P2) larger than 20° are not taken into account. The calculated slippage on the basis of Cg...Cg distances as well as the value of the angle between Cg...Cg vector and vertical line on corresponding plane has been taken into account as one of the geometrical criteria, too (approx. 1.5 Å for π···π stacking interactions).

[b] Rings Cg1,Cg3 and Cg4 are defined by the atoms N2, C1, C2, C3, C4 and C9; C10, C11, C12, C13, C14 and C15; C16, C17, C18, C19, C20 and C21, respectively.

[c] C_g···P1 is the perpendicular distance of corresponding centroid to a plane. Planes P1 or P2 are defined by the atoms, which define the corresponding centroids.

[d] C_g···P2 is the perpendicular distance of corresponding centroid to a plane. Planes P1 or P2 are defined by the atoms, which define the corresponding centroids.

[e] Dihedral angles between P1 and P2.

[f] β is the angle between Cg···Cg vector and vertical line on corresponding plane. Symmetry code: $i = 2 + x,1/2-y,3/2 + z$.

3.4. *Detection of different cations with compound **5***

The changes in fluorescence properties of compound **5** upon addition of different metal chloride salts were measured in ethanol at room temperature, at concentration 1×10^{-6} mol dm^{-3} of compound **5** while for the titration with Zn^{2+} cations the concentration of compound **5** was 5×10^{-7} mol dm^{-3}.

Stock solutions of various metal chloride salts ($ZnCl_2$, $MnCl_2$, $CuCl_2$, $CoCl_2$, $HgCl_2$, AgCl, LiCl and $FeCl_3$) were prepared in ethanol. Most of the results are presented in Fig. 8. As it can be viewed, the fluorescence intensity of compound **5** decreased in the presence of Mn^{2+}, Co^{2+}, Li^+ and Fe^{3+} cations while significantly increased upon addition of Zn^{2+} cation and Ag^+ cation. In Fig. 9. are presented summarized results of fluorescence response of compound **5** in the presence of all used cations at the same concentration of 1×10^{-6} mol dm^{-3} (Fig. 10).

In the presence of Hg^{2+} and Li^+ cations, the fluorescence intensity of compound **5** decreased. The highest fluorescence quenching of compound **5** was observed upon addition of Cu^{2+}

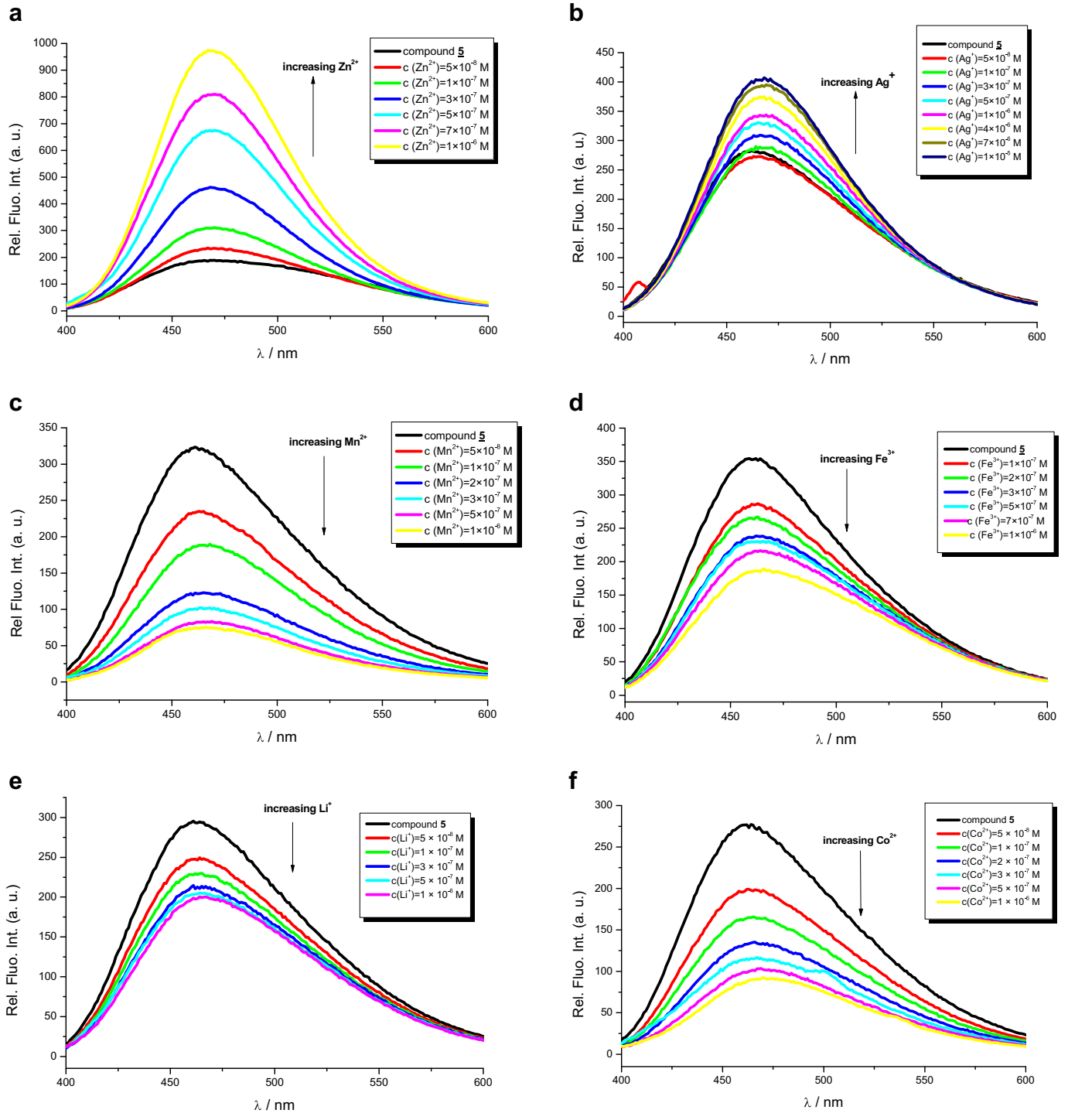

Fig. 8. Fluorescence intensity changes of compound **5** upon addition of different metal chloride salts in ethanol; a) Zn^{2+}; b) Ag^{+}; c) Mn^{2+}; d) Fe^{3+}; e) Li^{+}; f) Co^{2+}; ($\lambda_{exc} = 363$ nm).

cations (8 times). Moreover, the fluorescence maxima of compound **5** showed a slight red shift upon addition of Zn^{2+} (9 nm), Ag^{+} (7 nm), Hg^{2+} (9 nm), Co^{2+} (11 nm) and Cu^{2+} (14 nm).

The selectivity of chemosensor **5** towards different cations is presented in Fig. 11. After addition of the same amount of different cation solutions (30 μl, concentration of 1×10^{-6} mol dm^{-3}), respectively, only Zn^{2+} and Ag^{+} enhanced fluorescence emission at 460 nm for 3,51 and 1.46 times. All other cations quenched fluorescence emission at 460 nm Cu^{2+} almost totally quenched fluorescence at experimental conditions.

The changes in fluorescence intensity upon addition of different metal cations may be explained on the basis of a PCT mechanism (photoinduced charge transfer). As it is well known, when a fluorophore, which is benzimidazo[1,2-*a*]quinoline, is directly attached to an electron donating receptor, which is amino group, to form a new π-electron conjugation system which results in electron rich and electron poor terminals, it undergoes intramolecular charge transfer (ICT) from the donor to the acceptor upon excitation by light. Since a slight red shift in emission is observed, we could assume that an interaction between the

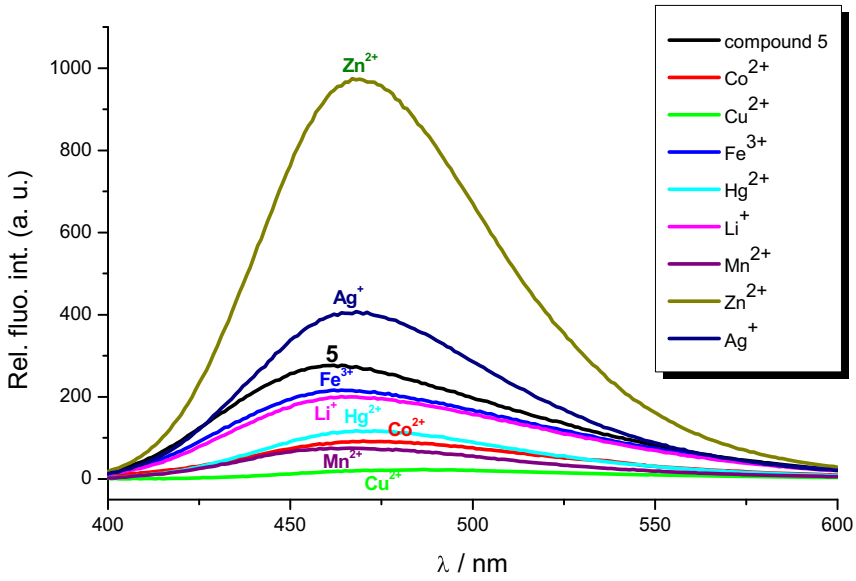

Fig. 9. Fluorescence response of compound **5** in the presence of different metal cations at the same concentration of 1×10^{-6} mol dm^{-3} in ethanol ($\lambda_{exc} = 363$ nm).

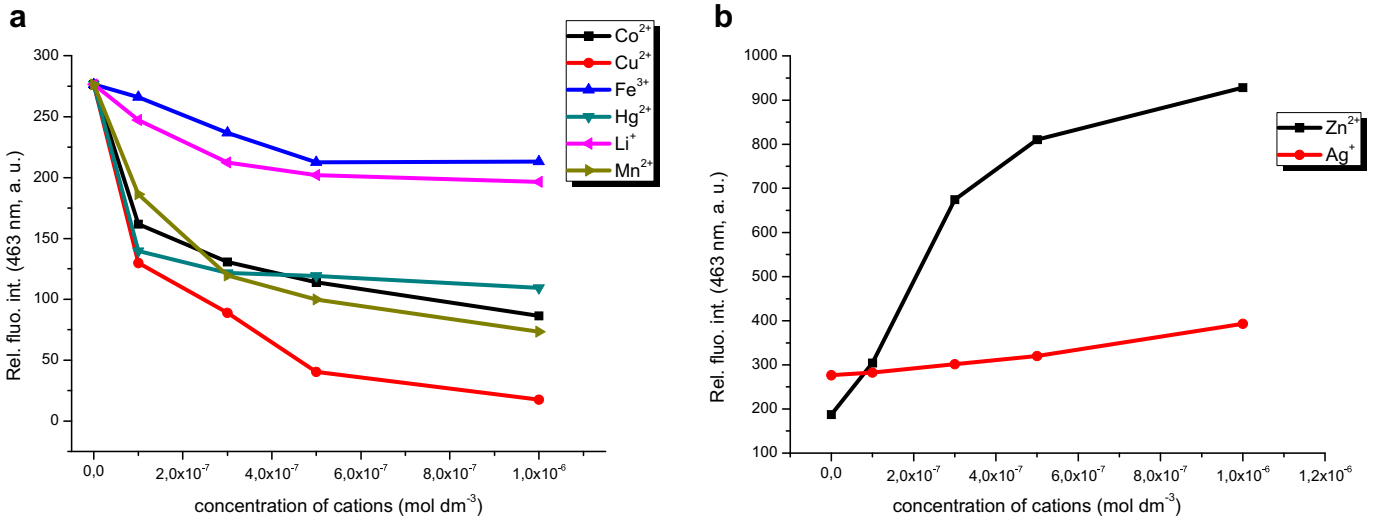

Fig. 10. Changes in fluorescence emission of compound **5** at 463 nm in the presence of different concentration of cations.

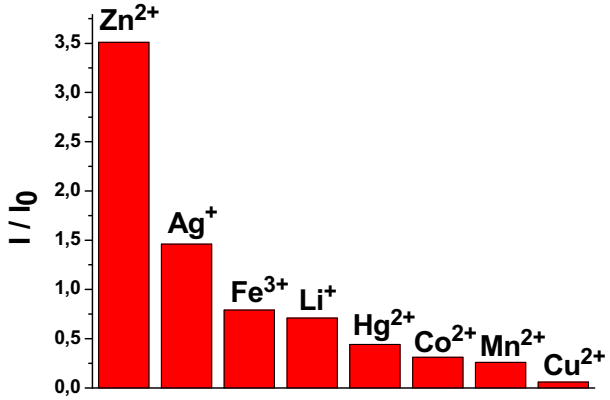

Fig. 11. The selectivity of chemosensor **5** towards different cations.

cation and receptor strengthens the push–pull effects and change the photophysical properties of fluorophore. To confirm our assumption, that amino group is responsible for interaction with cations, we have perform some additional experiments with 5-phenylbenzimidazo[1,2-*a*]quinoline-6-carbonitrile **4a**, unsubstituted derivative on quinoline nuclei, and 2-chloro-5-phenylbenzimidazo[1,2-*a*]quinoline-6-carbonitrile **4b.** Fluorimetric titrations with metal chloride salts of compounds **4a** and **4c** did not cause any significant changes in fluorescent intensities of compounds **4a** and **4c**.

4. Conclusion

In this work, we have presented the synthesis of novel *E*-3-phenyl-2-(1-phenyl-benzimidazol-2-yl)acrylonitriles **3a**–**3f** and

5-phenylbenzimidazo[1,2-*a*]quinolines **4a**–**4d**, **5** and **6**. All prepared compounds, especially the cyclic derivatives, showed interesting spectroscopic characteristic which were studied by UV/Vis and fluorescence spectroscopy in ethanol. Amongst all of the acyclic compounds, the nitro substituted compound **3d** showed an intense batochromic shift with emission maxima at 561 nm, while the cyclic compound **4a** showed the highest fluorescence intensity amongst all of the studied compounds. In comparison to unsubstituted **4a** and chloro substituted **4b** and **4c** benzimidazo[1,2-*a*] quinolines, nitro **4d** and amino **5** substituted compounds showed very low fluorescence quantum yield.

The crystal and molecular structures of two compounds **3d** and **4a** have been determined. Since the groups attached to C8 and C9 with the higher priority lie on the same side of a plane containing double C8 = C9 bond, the stereoisomer **3d** in the crystalline state is designated as *E*. The molecules are assembled in the crystal *via* weak C–H···O in **3d** and C–H···N intermolecular hydrogen bonds in **4a**.

To shed more light on the possibility of benzimidazo[1,2-*a*] quinolines for their application as a chemosensors for a variety of cations, amino substituted cyclic compound **5** was chosen for a spectroscopic study of its fluorescence properties in the presence of different metal chloride salts. Fluorescence emission spectra revealed that in the presence of Zn^{2+} and Ag^{+} cations, fluorescence intensity of compound **5** is significantly enhanced while in the presence of Mn^{2+}, Co^{2+}, Cu^{2+}, Hg^{2+}, Li^{+} and Fe^{3+} cations, fluorescence intensity is quenched. The observed changes together with bathochromic shifts of fluorescence intensity may be attributed to PCT process. Quinolines and its derivatives, despites of their disadvantages such as poor fluorescence or solubility, are well known fluorogenic chelators for transition metal ions and particularly for Zn^{2+} cation. Incorporation of benzimidazole nuclei with a quinoline units leads to improvement of photophysical properties. Thus, compound **5** showed special sensitivity for Zn^{2+} cation which could offer the possibility for its application for imaging and quantification Zn^{2+} in biological samples since, it is well known from the literature data that zinc is one of the most important transition metal ions in the human body, essential for the many biological processes such as brain function, gene transcription, immune function and mammalian reproduction [38].

Supplementary material

CCDC numbers 870440 & 870441 for compounds **3d** and **4a** respectively, contains the supplementary crystallographic data for this paper. These data can be obtained free of charge at www.ccdc.cam.ac.uk/conts/retrieving.html [or from the Cambridge Crystallographic Data Centre (CCDC), 12 Union Road, Cambridge CB2 1EZ, UK; fax: +44 (0)1223-336033; email: deposit@ccdc.cam.ac.uk]. Structure factors table is available from the authors.

Acknowledgments

This study was supported by grants 125-0982464-1356 and 098-1191344-2943 by the Ministry of Science, Education and Sports of the Republic of Croatia.

References

[1] Esteves CIC, Raposo MMM, Costa SPG. Synthesis and evaluation of benzothiazolyl and benzimidazolyl asparagines as amino acid based selective fluorimetric chemosensors for Cu2^{+}. Tetrahedron 2010;66:7479–86.
[2] Li Z, Zhang L, Li X, Guo Y, Ni Z, Chen J, et al. A fluorescent color/intensity changed chemosensor for Fe^{3+} by photo-induced electron transfer (PET) inhibition of fluoranthene derivative. Dyes and Pigments 2012;94:60–5.
[3] Jeong J, Yoon J. Recent progress on fluorescent chemosensors for metal ions. Inorganica Chimica Acta 2012;381:2–14.
[4] Boča M, Jameson RF, Linert W. Fascinating variability in the chemistry and properties of 2,6-bis-(benzimidazol-2-yl)-pyridine and 2,6-bis-(benzthiazol-2-yl)-pyridine and their complexes. Coordination Chemistry Reviews 2011; 255:290–317.
[5] Lee AE, Grace MR, Meyer AG, Tuck KL. Fluorescent Zn^{2+} chemosensors, functional in aqueous solution under environmentally relevant conditions. Tetrahedron Letters 2010;51:1161–5.
[6] Valeur B. Molecular fluorescence – principles and applications. Weinheim, Germany: Wiley-VCH; 2002.
[7] Valeur B, Leray I. Design principles of fluorescent molecular sensors for cation recognition. Coordination Chemistry Reviews 2000;205:3–40.
[8] Wu J, Liu W, Ge J, Zhang H, Wang P. New sensing mechanisms for design of fluorescent chemosensors emerging in recent years. Chemical Society Reviews 2011;40:348–95.
[9] de Silva AP, Gunaratne HQN, Gunnlaugsson T, Huxley AJM, McCoy CP, Rademacher JT, et al. Chemical Reviews 1997;97:1515–66.
[10] Demeunynck M, Bailly C, Wilson WD, editors. DNA and RNA binders. Weinheim: Wiley-VCH; 2002.
[11] Silverman RB. The organic chemistry of drug design and drug action. 2nd ed. Elsevier Academic Press; 2004.
[12] Ates-Alagöz Z, Alp M, Kus C, Yildiz S, Buyukbing E, Göker H. Synthesis and potent antimicrobial activities of some novel retinoidal monocationic benzimidazoles. Archiv der Pharmazie – Chemistry in Life Science 2006;339:74–80.
[13] Göker H, Özden S, Yıldız S, Boykin DW. Synthesis and potent antibacterial activity against MRSA of some novel 1, 2-disubstituted-1H-benzimidazole-N-alkylated-5-carboxamidines. European Journal of Medicinal Chemistry 2005; 40:1062–9.
[14] Hranjec M, Kralj M, Piantanida I, Sedić M, Šuman L, Pavelić K, et al. Novel cyano- and amidino-substituted derivatives of styryl-2-benzimidazoles and benzimidazo[1,2-a]quinolines. Synthesis, photochemical synthesis, DNA binding and antitumor evaluation, part 3. Journal of Medicinal Chemistry 2007;50:5696–711.
[15] Hranjec M, Piantanida I, Kralj M, Šuman L, Pavelić K, Karminski-Zamola G. Novel amidino-substituted thienyl- and furyl-vinyl-benzimidazole derivatives and their photochemical conversion into corresponding diaza-cyclopenta[c] fluorenes. Synthesis, interactions with DNA and RNA and antitumor evaluation. Part 4. Journal of Medicinal Chemistry 2008;51:4899–910.
[16] Perin N, Uzelac L, Piantanida I, Karminski-Zamola G, Kralj M, Hranjec M. Novel biologically active nitro and amino substituted benzimidazo[1,2-a]quinolines. Bioorganic and Medicinal Chemistry 2011;19:6329–39.
[17] Grogan HM. Fungicide control of mushroom cobweb disease caused by Cladobotryum strains with different benzimidazole resistance profiles. Pest Management Science 2006;62:153–61.
[18] Starčević K, Kralj M, Ester K, Sabol I, Grce M, Pavelić K, et al. Bioorganic and Medicinal Chemistry 2007;15:4419–26.
[19] Hirano K, Oderaotoshi Y, Minataka S, Komatsu M. Unique fluorescent properties of 1-aryl-3,4-diphenylpyrido[1,2-a]benzimidazoles. Chemistry Letters 2001:1262–3.
[20] Hoffmann HS, Stefani V, Benvenuttia EV, Haas Costaa TM, Russman Gallas M. Fluorescent silica hybrid materials containing benzimidazole dyes obtained by sol–gel method and high pressure processing. Materials Chemistry and Physics 2011;126:97–101.
[21] Langer R. Perspectives: drug delivery- drugs on target. Science 2001;293:58–9.
[22] Kovalska VB, Kryvorotenko DV, Balanda AO, Losytskyy MY, Tokar VP, Yarmoluk SM. Fluorescent homodimer styrylcyanines: synthesis and spectraleluminescent studies in nucleic acids and protein complex. Dyes and Pigments 2005;67:47–54.
[23] Lee DY, Singh N, Jang DO. A benzimidazole-based single molecular multianalyte fluorescent probe for the simultaneous analysis of Cu2^{+} and Fe3^{+}. Tetrahedron Letters 2010;51:1103–6.
[24] Li G, Gong WT, Ye JW, Lin Y, Ning GL. Unprecedented intramolecular cyclization of pyridinium to pyrido[1,2-a]benzimidazole: a novel chemodosimeter for fluoride ions. Tetrahedron Letters 2010;52:1313–6.
[25] Sahin C, Ulusoy M, Zafer C, Ozsoy C, Varlikli C, Dittrich T, et al. The synthesis and characterization of 2-(20-pyridyl)benzimidazole heteroleptic ruthenium complex: efficient sensitizer for molecular photovoltaics. Dyes and Pigments 2010;84:88–94.
[26] Hranjec M, Karminski-Zamola G. Synthesis of novel benzimidazolyl substituted acrylonitriles and amidino substituted benzimidazo[1,2-a]quinolines. Molecules 2007;12:1817–28.
[27] Hranjec M, Pavlović G, Marjanović M, Kralj M, Karminski-Zamola G. Benzimidazole derivatives related to 2,3-acrylonitriles, benzimidazo[1,2-a]quinolines and fluorenes: synthesis, antitumor evaluation in vitro and crystal structure determination. European Journal of Medicinal Chemistry 2010;45:2405–17.
[28] Perin N, Hranjec M, Pavlović G, Karminski-Zamola G. Novel aminated benzimidazo[1,2-a]quinolines as potential fluorescent probes for DNA detection: microwave-assisted synthesis, spectroscopic characterization and crystal structure determination. Dyes and Pigments 2011;91:79–88.
[29] Oxford Diffraction Ltd.. Xcalibur CCD system, CrysAlis software system. Version 1.171.34.40 Abingdon; Oxfordshire, England; 2008.
[30] Sheldrick GM. A short history of SHELX. Acta Crystallographica 2008;A64:112–22.
[31] Farrugia LJ. WinGX suite for small-molecule single-crystal crystallography. Journal of Applied Crystallography 1999;32:837–8.

[32] Spek L. A multipurpose crystallographic tool. Journal of Applied Crystallography 2003;36:7–13.
[33] Nardelli M. PARST95-an update to PARST: a system of Fortran routines for calculating molecular structure parameters from the results of crystal structure analyses. Journal of Applied Crystallography 1995;28:659.
[34] Farrugia LJ. Ortep-3 for Windows (v. 2.02) - a version of the current release of ORTEP-III, which incorporates a Graphical User Interface (GUI). Journal of Applied Crystallography 1997;30:565.
[35] http://www.povray.org/.
[36] Macrae CF, Bruno IJ, Chisholm JA, Edgington PR, McCabe P, Pidcock E, et al. Mercury CSD Ver. 2.0. - new features for the visualization and investigation of crystal structures. Journal of Applied Crystallography 2008;41:466–70.
[37] Hranjec M, Pavlović G, Karminski-Zamola G. Crystal structure and synthesis of benzimidazole substituted acrylonitriles and benzimidazo[1,2-a]quinolines. Structural Chemistry 2009;20:91–9.
[38] Xu Z, Yoon J, Spring DR. Fluorescent chemosensors for Zn^{2+}. Chemical Society Review 2010;39:1996–2006.